Supplementary Material to "On the non-uniqueness of sediment yield at the catchment scale: the effects of soil antecedent conditions and surface shield"

Jongho Kim[1] and Valeriy Y. Ivanov[1]

[1]Department of Civil and Environmental Engineering

University of Michigan, Ann Arbor, MI 48103

December 8, 2013

Corresponding author: Jongho Kim, Department of Civil and Environmental Engineering, University of Michigan, Ann Arbor, MI 48103, tel (734) 763-9663, email: kjongho@umich.edu.

SM.1. Relative contributions of erosion sources to total erosion

In field studies, overland flow-driven erosion (i.e., entrainment and reentrainment) would be expected to dominate rainfall-induced erosion (i.e., detatchment and redetachment). To illustrate whether the adopted parameter set can represent such a condition, the time series of spatially-averaged rates of four erosion sources are shown in Figure SM.1 for one of the rainfall events, RI_1 = 50 mm/hr of Case 5. It indicates that the reentrainment rate is the most significant contributor to erosion, exceeding the redetachment rate by a factor of two.

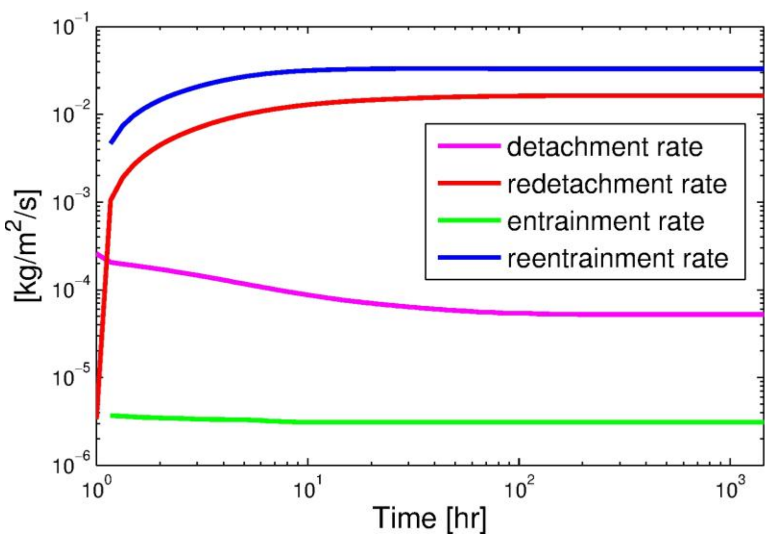

Figure SM.1. The time series of spatially-averaged rates of detachment, redetachment, entrainment, and reentrainment for the rainfall intensity of 50 mm/hr (Case 5).

SM.2. Temporal distributions of morphologic variables for different rainfall intensities and particle sizes, and two time scales

For five rainfall intensities and four particle sizes, Figure SM.2 illustrates the dynamic unsteady evolution of three morphologic variables: sediment concentration (C_{hr}^{ini}) and deposited mass (M_{hr}^{ini}) averaged over the basin at every hour as well as hourly sediment yield (SY_{hr}) for the entire simulation period. A qualitative interpretation of this figure reveals that similarly to the results for the total concentration and deposited mass (subplots in column (a)), the hourly, size-specific series of SY_{hr} are in accordance with the series of C_{hr}^{ini} and M_{hr}^{ini} for S1, S2, and S3 particle sizes, while they are dissimilar for S4. Additionally, higher contributions of either concentration or deposited mass to their total can be detected for either smaller or larger particles, respectively.

Based on the criteria formulated in Eq. (2), both the time to peak (t_1) and the time to steady state (t_2) were computed and illustrated in all sub-plots (see the two vertical dotted lines in most of the sub-plots). The characteristics associated with these critical times are as follows. (1) The larger the rainfall forcing, the shorter the time intervals to peak and the steady state. (2) The results for the smallest RI_1=10 mm/hr show that the steady state is not reached within the simulation period of 60 days. (3) The patterns of temporal dynamics of sediment variables vary depending on the particle size; specifically, as the size of soil particle increases, t_1 and t_2 also increase. (4) For S4, SY_{hr} approaches the steady state magnitude coincides with the peak, which implies that the values of t_1 and t_2 are equal.

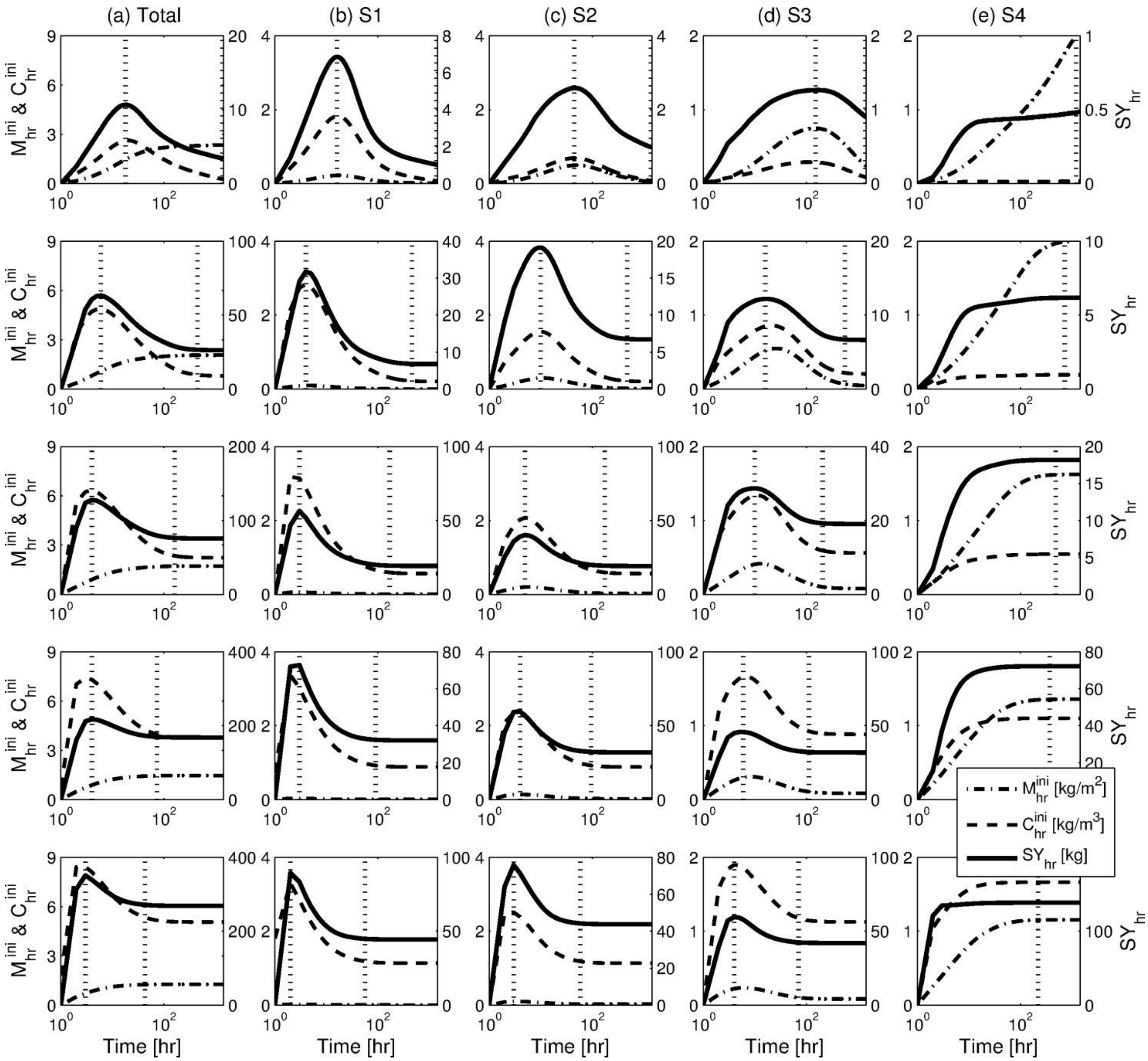

Figure SM.2. The time series of spatially-averaged concentration (C_{hr}^{ini}), deposited mass (M_{hr}^{ini}), and the outlet sediment yield (SY_{hr}) as bulk characteristics (column a) and specific for each particle size (columns b, c, d, and e). Simulation results are for Case 5. The five sub-plots in the same row correspond to the same rainfall intensity: from 10 mm/hr in the top row, to 90 mm/hr in the bottom row. In each sub-plot, the left axis is used for M_{hr}^{ini} and C_{hr}^{ini}, while the right axis is used for SY_{hr}. Two vertical dotted lines represent the time to peak (t_1) and the time at steady state (t_2), respectively.

SM.3. Effects of rainfall intensity on $C_{i,hr}^{ini}$ and $M_{i,hr}^{ini}$

For five rainfall intensities of 10, 30, 50, 70, and 90 in Case 5, the cumulative SY_{hr}^{cum} is illustrated with respect to the spatially-averaged C_{hr}^{ini} (Figure SM.3-(a)) and M_{hr}^{ini} (Figure SM.3-(b)) corresponding to four particle sizes (S1 to S4). Interesting features associated with different rainfall intensities are: (1) the maximum absolute deviation between the concentrations or deposited masses corresponding to different particle sizes (i.e., $|C_{4,hr}^{ini} - C_{1,hr}^{ini}|$ or $|M_{4,hr}^{ini} - M_{1,hr}^{ini}|$) occurs for the smallest rainfall intensity. This signifies that smaller runoff rate allows a wide range of particle size distributions, either near the beginning of runoff generation (for concentrations) or during the steady state (for deposited mass). Conversely, a nearly uniform PSD occurs initially for $M_{i,hr}^{ini}$, resembling the PSD of the original, ‘intact’ soil; this is more pronounced for the smaller *RI*. Such an effect occurs because smaller eroding or transporting power of smaller *RI* takes longer time to alter the original soil into ‘loose’ soil and to initiate size-selective erosion processes. Similarly, a uniform PSD for $C_{i,hr}^{ini}$ is observed when the steady state is achieved.

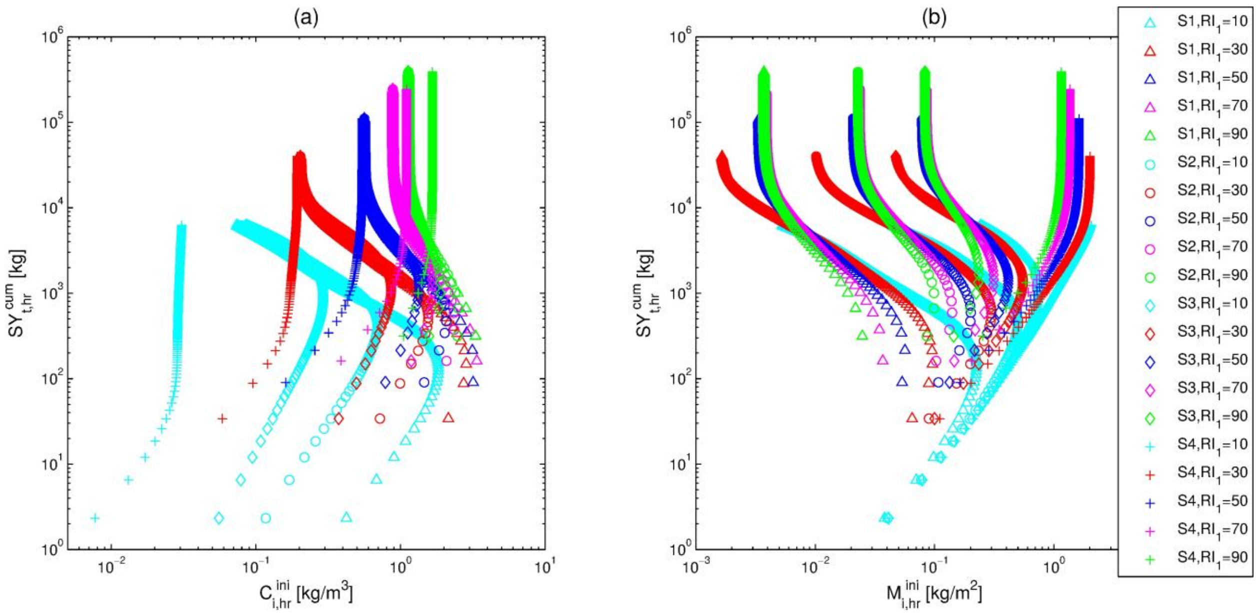

Figure SM.3. The cumulative total sediment yield resolved at the hourly scale ($SY_{t,hr}^{cum}$) versus the hourly instantaneous, spatially-averaged (a) concentrations ($C_{i,hr}^{ini}$) and (b) deposited mass ($M_{i,hr}^{ini}$) corresponding to four particle sizes (S1 to S4) and five rainfall intensities ($RI_{1,}$) of 10, 30, 50, 70, and 90 for Case 5.

Table SM.1. The range of parameter values reported in literature using the Hairsine-Rose model. Depending on whether a study focused on either rainfall- or flow- driven erosion problem, only a single set of erosion parameters can be reported.

Studies	a_0[kg/m^3]	a_d [kg/m^3]	F [-]	Ω_{cr} [W/m^2]	J [m^2/s^2]	$M_t{}^*$ [kg/m^2]
Proffitt et al. (1991)	15-110	40-250	-	-	-	-
Sander et al. (1996)	319-3910	3705-24660	-	-	-	0.05-0.23
Hogarth et al. (2004a)	920-2300	1419-4370	-	-	-	0.0767-0.273
Gao et al. (2005)	400	-	-	-	-	5-8.7
Tromp-van Meerveld et al. (2008)	21.7	6510	-	-	-	0.16
Jomma et al. (2010)	9.1-94	5246-13842	-	0.15-0.2	-	0.004-0.08
Jomma et al. (2012)	5.5-27	8000-28000	-	-	-	0.025-0.11
Jomma et al. (2013)	1.1-12	10000-28000	-	-	-	0.025-0.05
Proffitt et al. (1993)	-	-	0.1	-	<30	-
Misra and Rose (1995)	18.2-129.7	12000-76300	0.18-0.25	0.007	4.5-133.3	-
Beuselinck et al. (2002)	-	0-225000	0.0013	0.185-0.2	-	H=1
Hairsine et al. (2002)	-	-	0.0075	0.185	-	-
Sander et al. (2002)	-	-	0.01	0.18639	-	H=1
Van Oost et al. (2004)	-	-	0.013	0.6	-	H=1
Rose et al. (2007)	-	-	0.0246-0.109	0.01	0.0737-0.632	0.0351-0.626
Heng et al. (2011)	9-27	1900	0.01-0.02	0.00012-0.00019	555-1666	1.5-5
Kim et al. (2013)	80	2000	0.01	0.12	189	2.7

This study	20	2000	0.01	0.07-0.17	750	2.7

References

Beuselinck, L., G. Govers, P. B. Hairsine, G. C. Sander, and M. Breynaert (2002), The influence of rainfall on sediment transport by overland flow over areas of net deposition, *Journal of Hydrology*, *257*(1-4), 145-163.

Gao, B., M. T. Walter, T. S. Steenhuis, J. Y. Parlange, B. K. Richards, W. L. Hogarth, and C. W. Rose (2005), Investigating raindrop effects on transport of sediment and non-sorbed chemicals from soil to surface runoff, *Journal of Hydrology*, *308*(1–4), 313-320.

Tromp-van Meerveld, H. J., J. Y. Parlange, D. A. Barry, M. F. Tromp, G. C. Sander, M. T. Walter, and M. B. Parlange (2008), Influence of sediment settling velocity on mechanistic soil erosion modeling, *Water Resources Research*, *44*(6).

Van Oost, K., L. Beuselinck, P. B. Hairsine, and G. Govers (2004), Spatial evaluation of a multi-class sediment transport and deposition model, *Earth Surface Processes and Landforms*, *29*(8), 1027-1044.